Tuning the two-dimensional electron gas at the LaAlO_{3}/SrTiO_{3}(001) interface by metallic contacts

Rémi Arras, Victor G. Ruiz, Warren E. Pickett, and Rossitza Pentcheva

Phys. Rev. B **85**, 125404 — Published 5 March 2012

DOI: 10.1103/PhysRevB.85.125404

Tuning the two-dimensional electron gas at the $LaAlO_3/SrTiO_3$(001) interface by metallic contacts

Rémi Arras,[1] Victor G. Ruiz,[1] Warren E. Pickett,[2] and Rossitza Pentcheva[1,*]

[1]*Department of Earth and Environmental Sciences, Section Crystallography and Center of Nanoscience, University of Munich, Theresienstr. 41, 80333 Munich, Germany*

[2]*Department of Physics, University of California, Davis, One Shields Avenue, Davis, CA 95616, U.S.A.*

Density functional theory calculations reveal that adding a metallic overlayer on $LaAlO_3/SrTiO_3$(001) alters significantly the electric field within the polar $LaAlO_3$ film. For Al or Ti metal contacts the electric field is eliminated, leading to a suppression of the thickness-dependent insulator-to-metal transition observed in uncovered films. Independent of the $LaAlO_3$ thickness, both the surface and the interface are metallic, with an enhanced carrier density at the interface relative to $LaAlO_3/SrTiO_3$(001) after the metallization transition. Monolayer thick contacts of Ti develop a finite magnetic moment and for a thin $SrTiO_3$ substrate induce a spin-polarized two-dimensional electron gas at the *n*-type interface, due to confinement effects in the $SrTiO_3$ slab. For transition and noble metal contacts (Cu, Ag, Au) a finite and even enhanced (Au) internal electric field develops within $LaAlO_3$. Results for a representative series of metallic overlayers on $LaAlO_3/SrTiO_3$(001) (Na, Al; Ti, Fe, Co, Pt; Cu, Ag, Au) reveal broad variation of band alignment, size of Schottky barrier and carrier concentration at the $LaAlO_3/SrTiO_3$(001) interface. The identified relationship to the size of work function of the metal on $LaAlO_3$ provides guidelines how the carrier density at the $LaAlO_3/SrTiO_3$ interface can be controlled by the choice of the metal contact.

PACS numbers: 73.20.-r,71.30.+h,73.40.Qv,77.55.-g

I. INTRODUCTION

The (001) interface between the band insulators $LaAlO_3$ (LAO) and $SrTiO_3$ (STO) provides remarkable examples of novel functionalities that can arise at oxide interfaces, including a two-dimensional electron gas (2DEG)[1], superconductivity[2], magnetism[3] and even signatures of their coexistence[4–6]. A further intriguing feature is the thickness-dependent transition from insulating to conducting behavior in thin $LaAlO_3$ films on $SrTiO_3$(001) at $\sim$ 4 monolayers (ML) LAO[7]. This insulator-to-metal transition (MIT) can be controlled reversibly via an electric field, e.g. by an atomic force microscopy (AFM) tip[8–10] or by an additional STO capping layer that can trigger the MIT already at 2 ML of LAO and thereby stabilize an electron-hole bilayer[11]. Density functional theory calculations (DFT) have demonstrated the emergence of an internal electric field for thin polar LAO overlayers[12–15]that is partially screened by a strong lattice polarization in the LAO film[13,16]. This lattice screening allows several layers of LAO to remain insulating before an electronic reconstruction takes place at around 4-5 monolayers of LAO. Recent AFM experiments provide evidence for such an internal field in terms of a polarity-dependent asymmetry of the signal[17], but x–ray photoemission studies[18–20] have not been able to detect shifts or broadening of core-level spectra that would reflect an internal electric field. This discrepancy implies that besides the electronic reconstruction, extrinsic effects play a role, e.g. oxygen defects[21,22], adsorbates such as water or hydrogen[23] or cation disorder[24,25] (for detailed reviews on the experimental and theoretical work see[14,26–28]).

The LAO/STO system is not only of fundamental scientific interest, but is also a promising candidate for the development of electronics and spintronics devices[29,30]. For its incorporation in such devices the influence of metallic leads needs to be considered[31–33]. Metallic overlayers have been investigated on a variety of perovskite surfaces, such as $SrTiO_3$(001)[34,35], $LaAlO_3$(001)[36,37] or $BaTiO_3$(001)[38,39]. A further area of research is the magnetoelectric coupling between ferromagnetic Fe and Co films and ferroelectric $BaTiO_3$ and $PbTiO_3$(001)-surfaces[40,41]. However, the impact of a metallic overlayer on a buried oxide interface has not been addressed so far theoretically.

Density functional theory calculations for Ti as an example for a conventional metal contact, show that it not only provides a Schottky barrier, but also has a crucial influence on the electronic properties of LAO/STO(001) as it removes the internal electric field in the LAO film. Despite the lack of a potential build up in the LAO layers, the underlying STO layer is metallic with a significantly enhanced carrier concentration at the n-type interface as compared to the system without metallic contact. Although bulk Ti is nonmagnetic, the undercoordinated Ti in the contact layer shows an enhanced tendency towards magnetism with a significant spin polarization and a magnetic moment of 0.60 μ_B. Most interestingly, quantum confinement within the STO-substrate can induce spin-polarized carriers at the interface. Furthermore, the influence of the Ti contact layer thickness and the thermodynamic stability are addressed.

Besides Ti in Section IV we extend our study to a variety of metallic contacts: Al and Na as simple metals; Fe, Co and Pt to supplement the Ti study and show the variations occurring within the class of transition metals and finally, the noble metals Cu, Ag, and Au, that display a remarkably different behavior. These results demonstrate that the properties of LAO/STO(001) can be tuned by the choice of metal contact and we identify the mechanisms associated with these broad variations in characteristics.

II. CALCULATIONAL DETAILS

DFT calculations on nM/mLAO/STO(001) were performed using the all-electron full-potential linearized augmented plane wave (FP-LAPW) method in the WIEN2k implementation[42] and the generalized gradient approximation (GGA)[43] of the exchange-correlation potential. Here n/m denotes the number of metallic overlayer/monolayers of LAO and M is the type of metallic contact. We have tested the influence of an on-site Coulomb correction within the LDA/GGA+U approach[44] with $U = 5$ eV and $J = 1$eV applied on the Ti $3d$-states within STO and $U = 7$ eV on the La $4f$ states and found only small differences in the electronic behavior (see Section III). In order to avoid the emergence of a spurious electric field due to the periodic boundary conditions, we have chosen a symmetric slab with LAO and Ti layers on both sides of the STO-substrate and a vacuum region between the slab and its periodic images of at least 10Å. The lateral lattice parameter is set to the GGA equilibrium lattice constant of STO (3.92 Å, slightly larger than the experimental value 3.905 Å) and the atomic positions are fully relaxed within tetragonal symmetry. To investigate the influence of the STO-substrate thickness we have used two cases with 2.5 ML and 6.5 ML STO (denoted as thin and thick). As will be shown below, we observe interesting effects due to confinement in the STO part of the slab.

III. INFLUENCE OF A TI CONTACT ON LAO/STO(001)

A. Thin STO substrate: quantum confinement effects

Fig. 1a shows the layer resolved density of states (LDOS) of a single Ti overlayer on 4ML LAO/STO(001) [1Ti/4LAO/STO(001)], where the Ti atoms are adsorbed on top of the oxygen ions in the surface AlO_2 layer. A striking feature is that the electric field of the uncovered LAO film (black line), expressed in an upward shift of the O $2p$ bands and unoccupied La $4f$ states[13], is eliminated after the adsorption of the Ti overlayer. In contrast to the insulator-metal transition that occurs in the uncovered LAO/STO(001), no dependence of the electronic properties on the LAO thickness is expected due to the vanishing electric field within the LAO layer. Indeed the LDOS of 1Ti/2LAO/STO(001) (Fig. 1b, only 2 LAO layers) confirms a very similar behavior with no shifts of the O $2p$ bands in the LAO part. Despite the lack of a potential build up, there is a considerable occupation of the Ti $3d$ band at the interface and thus both the surface Ti layer and the interface are metallic. This points to a charge transfer from the Ti adlayer allowing the Ti+LAO+STO system to equilibrate in charge and potential, with the result being that the Fermi level lies just within the STO conduction band.

The low coordination of the surface Ti atoms enhances their tendency towards magnetism resulting in a magnetic moment of $0.60\mu_{\rm B}$ in the surface layer. The electron gas at the interface is also spin-polarized with magnetic moments sensitive to the thickness of the LAO-spacer: for $m_{LAO} = 4$ the magnetic moments are smaller ($0.05/0.11\mu_{\rm B}$ in the interface (IF)/IF-1 layer) than for $m_{LAO} = 2$ ($0.10/0.24\mu_{\rm B}$ in IF/IF-1). Calculations performed within GGA+U for the latter case show a similar behavior but with an enhanced spin-polarization of carriers and magnetic moments of Ti of 0.20/0.30 $\mu_{\rm B}$ in the IF/IF-1 layer, respectively. Thus correlation corrections have only small influence on the overall band alignment, showing that the observed behavior is not affected by the well known underestimation of band gaps of LDA/GGA.

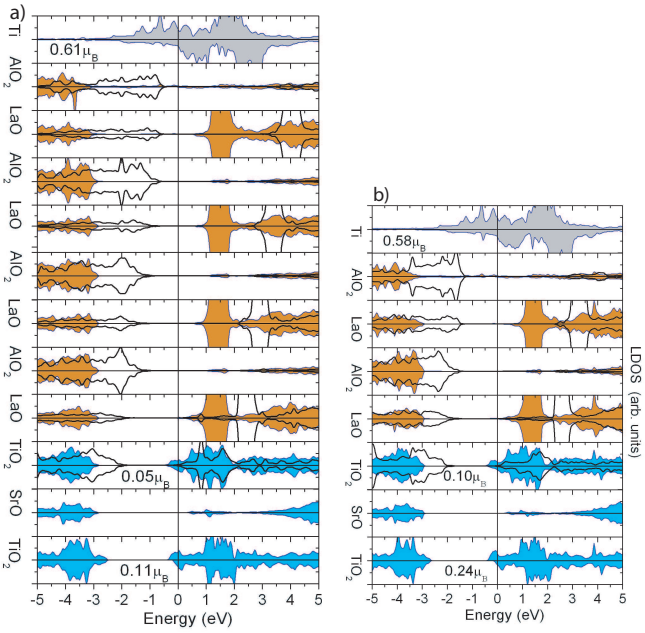

FIG. 1: (Color online) Layer resolved density of states (LDOS) of a) 1Ti/4LAO/STO(001) and b) 1Ti/2LAO/STO(001) (with thin STO substrate). The potential build up in the uncovered systems (black line) is canceled in the ones with a Ti overlayer (filled area). Additionally, there is a significant spin-polarization both in the surface Ti, as well as the interface TiO_2 layers in 1Ti/NLAO/STO(001).

B. Thick STO substrate: orbital polarization of carriers

The calculations so far were performed with a rather thin substrate layer of 2.5 ML STO. To examine the dependence on the thickness of the substrate layer, we studied 1Ti/2LAO/STO(001) containing a 6.5 ML thick STO part. As shown in Fig. 2a, the most prominent difference to the system with a thin STO layer is the suppression of magnetic moment of carriers at the interface, indicating that the spin-polarization is a result of confinement effects in the thin STO layer. Apart from this, a notable band bending occurs in the STO part of the heterostructure. The largest occupation of the Ti $3d$ band arises at the LAO/STO(001) interface, followed by a decreasing occupation in deeper layers. The electron density, integrated over states between $\rm E_F - 0.5$eV and $\rm E_F$ in Fig. 2b, reveals orbital polarization of the Ti $3d$ electrons in the conduction band with predominantly d_{xy} character in the interface layer, nearly degenerate t_{2g} occupation in IF-1, and a

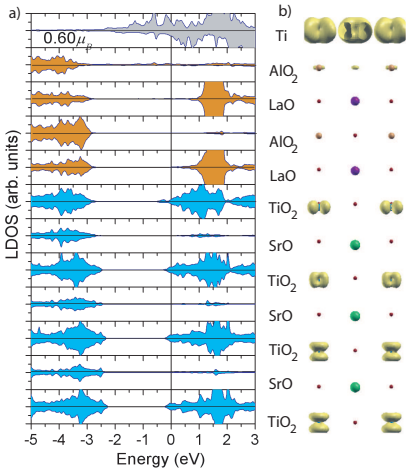

FIG. 2: (Color online) a) Layer resolved density of states (LDOS) of 1Ti/2LAO/STO(001) within GGA with a 6.5ML thick STO-substrate; b) Side view of the system with the electron density integrated in the interval $E_F - 0.5$eV to E_F, giving insight into the Ti $3d$ orbital occupation both at the surface and within $SrTiO_3$.

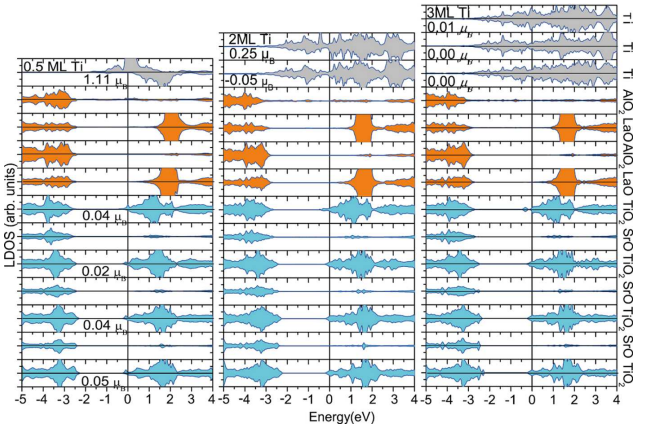

FIG. 3: (Color online) Layer resolved density of states (LDOS) of 0.5, 2 and 3 ML To on 2LAO/STO(001) within GGA with a 6.5ML thick STO-substrate, showing similar band alignment as for 1Ti/2LAO/STO(001) (cf. Fig. 2) as well as a reduction of spin-polarization of Ti in the contact layer with increasing thickness.

preferential occupation of d_{xz}, d_{yz} levels in the deeper layers. The band structure plotted in Fig. 6 shows that the conduction band minimum is at the Γ-point, formed by d_{xy} states of Ti in the interface TiO_2-layer. While the d_{xy} bands have a strong dispersion, the d_{xz}, d_{yz} bands lie slightly higher in energy but are much heavier along the $\Gamma - X$ direction. In addition to the orbital polarization of the filled bands, the different band masses indicate a significant disparity in mobilities of electrons in the different t_{2g} orbitals. Similar multiple subband structure has been recently reported for LAO/STO superlattices[45,46], δ-doped LAO in STO[47] as well as doped STO(001)-surfaces[48,49]. The remaining bands between -2.5eV and E_F are associated with the surface Ti-layer.

C. Effect of the Ti-contact layer thickness

In order to explore the effect of metallic contact thickness n we have performed calculations varying the Ti-amount in the contact layer between 0.5 and 3 ML. The layer resolved DOS for those cases is shown in Fig. 3. While the overall band alignment within LAO/STO(001) remains nearly unchanged, the main effect observed is the broadening of the Ti-bands in the contact layer as n increases. The enhanced coordination number within the contact layer influences significantly the tendency towards spin-polarization: the highest spin-polarization is observed for 0.5ML Ti (1.11μ_B), followed by 1ML Ti (0.60μ_B) (for comparison, the magnetic moment of a free standing Ti layer is 0.90μ_B). Increasing the thickness of Ti to 2 ML (with Ti in the second layer positioned above Al in the surface AlO_2-layer and La in the subsurface LaO-layer) leads to a significant reduction of the spin-polarization of the Ti film: the magnetic moment is 0.25μ_B in the surface and -0.10μ_B in the subsurface layer. Finally, in the 3ML-thick contact the magnetization of Ti is quenched.

The Ti-O bond length reflects the bonding strength between the contact layer and the oxide and varies with thickness: the shortest Ti-O bond length is in 0.5 ML Ti/2LAO/STO(001) (1.87 Å), followed by 1 ML Ti (2.00Å) and much longer in 2 and 3 ML Ti on 2LAO/STO(001) (2.06 Å and 2.05 Å, respectively). Despite these differences in the structural and magnetic properties of the metallic overlayer, the occupation of the Ti $3d$ band at the interface is very similar (cf. Fig. 4b), but decreases quicker in deeper layers within STO for 2 ML Ti.

An interesting effect concerns the structural relaxations in LAO/STO(001) upon deposition of the metal overlayer. The layer resolved anion-cation buckling is shown in Fig. 4a. As mentioned above, the system without electrodes (orange line) exhibits a strong lattice polarization within LAO, dominated by an outward relaxation of the cations, and a negligible polarization within the STO-substrate[13]. Adding the Ti overlayer cancels the lattice polarization within LAO, but a significant polarization emerges within STO which is strongest at the interface and decreases in deeper layers. The formation of a dipole in STO goes hand in hand with the occupation/band-bending of the Ti $3d$ bands displayed in Fig. 4b and Fig. 3, respectively. Furthermore, the layer resolved occupation of the Ti $3d$ band correlates with the positions of O$1s$ core levels with respect to the Fermi level (cf. Fig. 4c). The lowest O$1s$ eigenvalue occurs at the interface, with the strongest binding energy in the case of a Ti monolayer with a thin STO substrate (occupation of $0.2e$ of the Ti $3d$ orbitals). In the systems with a thick STO-substrate the O1s levels in deeper layers away from the IF shift upwards and converge to a similar value indicative of the relaxation of the inner potential towards the bulk STO value.

Thermodynamic stability. Besides the electronic properties of Ti contacts an important aspect is whether the surface will be wetted by the metallic overlayer. We find that the ordered surface distribution of 0.5 ML Ti is energetically strongly dis-

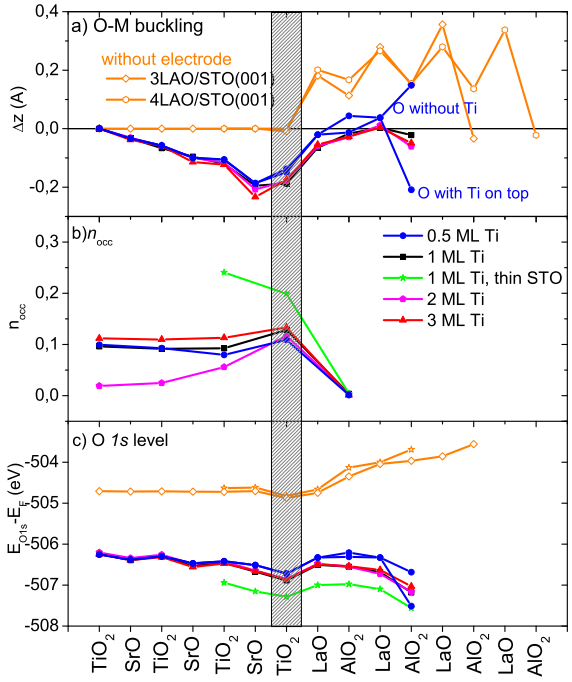

FIG. 4: (Color online) a) Cation-anion buckling Δz in nTi/2LAO/STO(001), n=0.5-3 ML. Note that the strong lattice polarization within LAO for 3 and 4 ML LAO/STO(001) is strongly suppressed once the metallic contact is added; b) Layer resolved Ti $3d$ band occupation integrated between $E_F - 0.65$ eV and E_F for M/2LAO/STO(001) 1ML Ti and thin (green stars)/thick STO substrate (black squares); 2ML Ti (magenta diamonds), as well as 1ML Pt (blue triangles) and 1ML Al (red circles). b) Positions of O1s states with respect to E_F. In 0.5 ML Ti, there are two different oxygen sites in the top AlO_2 layer with and without Ti on top that exhibit different properties.

favored by 1.84 eV with respect to the formation of 1ML high Ti islands covering 50% of the surface. On the other hand the formation of a closed 1ML Ti film is 0.54 eV less stable than the formation of 2ML islands on the LAO/STO(001) surface. No further energy gain is obtained for the growth of higher, e.g. 3ML islands, indicating that already the 2ML islands are thermodynamically stable. We note that using state-of-the-art techniques like molecular beam epitaxy and pulsed layer deposition it is possible to grow metal monolayers away from thermodynamic equilibrium.

IV. TRENDS FOR DIFFERENT METALLIC CONTACTS

Besides Ti, we have extended our study to a variety of metallic contacts ranging from simple metals as Al and Na, to transition metals (Fe, Co, Pt) and noble metals (Cu, Ag and Au). The results are summarized in Table I and displayed in

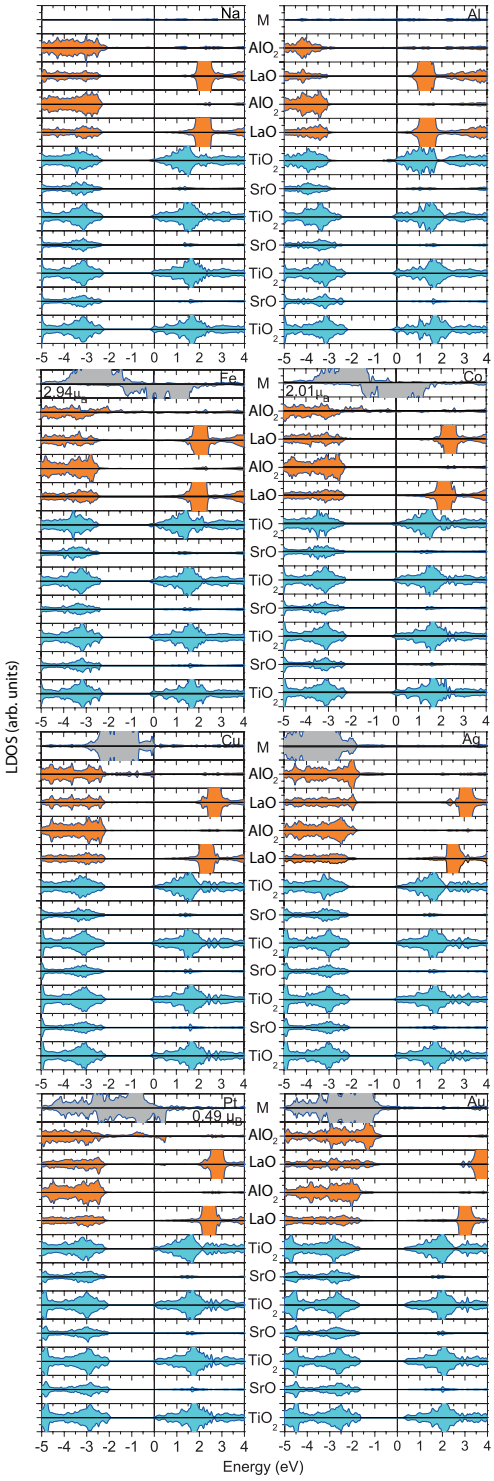

FIG. 5: (Color online) Layer resolved DOS of M/2LAO/STO(001), M=Al, Fe, Co, Cu, Ag, Pt and Au monolayer thick contacts. Note that the internal electric field in the LAO film is canceled for Na and Al, strongly suppressed but increasing in the series from Fe to Pt and significantly enhanced compared to the uncovered film for an Au contact.

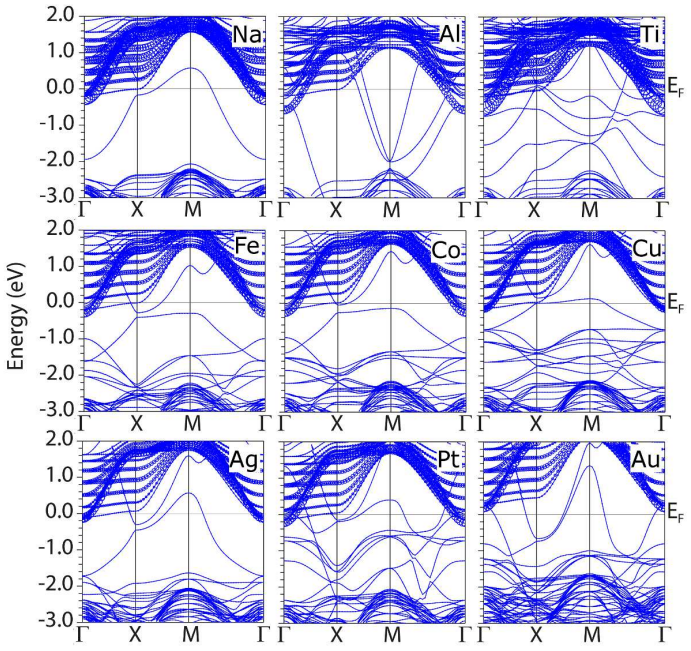

FIG. 6: Majority-spin band structures for Al, Ti, Fe, Co, Cu, Ag, Pt and Au contacts. The Ti $3d$ bands in the interface TiO_2-layer are emphasized by circles with the d_{xy} orbital being the lowest lying level at Γ. The highest occupation of the Ti $3d$ band at the LAO/STO(001) interface is observed for an Al contact and decreases in the series. Finally, for Au it lies even above the Fermi level.

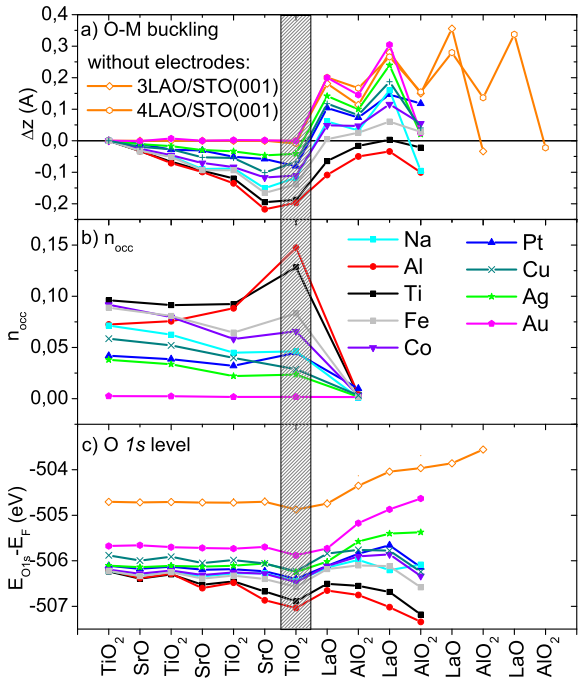

FIG. 7: a) Cation-anion buckling Δz in M/2LAO/STO(001). Note that the strong lattice polarization within LAO for 3 and 4 ML LAO/STO(001) is strongly suppressed once the metallic contact is added; b) Layer resolved Ti $3d$ band occupation integrated between $E_F - 0.65$ eV and E_F for M/2LAO/STO(001) 1ML Ti and thin (green stars)/thick STO substrate (black squares); 2ML Ti (magenta diamonds), as well as 1ML Pt (blue triangles) and 1ML Al (red circles). Note that charge on the AlO_2 layer next to the interface is nearly vanishing in all cases, charge on the AO layers is zero (not shown). b) Positions of O$1s$ states with respect to E_F.

Figs. 5-7. While the most striking behavior seen for the Ti contact – strong reduction, in fact almost perfect cancellation of the electric field within LAO and a formation of a 2DEG at the LAO/STO interface – might be expected for all electrodes, we will demonstrate broad variation in these features.

Variation in the spectrum. The LDOS plots in Fig. 5 show that the potential buildup within LAO is eliminated for Al as was found for Ti. For the case of Fe there is a small electric field in LAO, visible in upward shifts of the empty La $4f$ bands in subsequent layers towards the surface, which becomes successively larger for Co and Pt (and of the same sign as for the uncapped LAO surface). Note that in these systems the O $2p$ bands within LAO do not shift, instead metal induced gap states appear in the topmost AlO_2 layer. Evidently there is no necessity for a vanishing electric field in LAO. For Cu, Ag and especially for Au contacts, the field in LAO is large. For Au it is even *larger* than for the uncovered surface (0.85 vs. 0.65 eV per LAO cell). Thus the metal contact layer need not eliminate the field in LAO; it most often reduces it, sometimes strongly; in contrast, for Au, the internal field in LAO is *enhanced*.

Carriers at the interface. The highest Ti $3d$ band occupation (largest electronic carrier density) at the interface (see Fig. 7b) is found for an Al contact, followed by Ti, Fe, Co, Cu and Pt contacts, and then Ag exhibits the lowest occupation. The system with an Au contact is an exception as the Ti $3d$ band at the interface remains above the Fermi level (see Fig. 6). With the Fermi level of Au within the STO gap, charge transfer between Au and the interface is precluded. The Au contact provides the limiting case of vanishing charge exchange between metal and interface, though the surface and the interface may still be coupled in other ways, *i.e.* through the potentials, which depend on band lineups and dipole layers.

As mentioned already for Ti contacts, the trends in Ti $3d$ band occupation within STO correlate with the position of O $1s$ states: The O $1s$ binding energy is highest in the interface TiO_2-layer in case of an Al contact and lowest for an Au contact (cf. Fig. 7c). These quantitative differences are associated with variations in the chemical bond between the metal overlayer and the surface AlO_2 layer: *e.g.* the bonding is strongly ionic in the case of Na and Al with a significant charge transfer from the metal to O and is much weaker for a Cu, Pt, Ag and Au overlayer. There is also a sizable change in bond distances within the series from 1.97Å (Al) to 3.05Å (Au) (see

TABLE I: Properties of nM/2LAO/STO(001) with n ML of metallic contact M: Bond length distance $d_{M-\mathrm{O}}$ between the metallic contact and oxygen in the top AlO_2 layer, buckling Δz and Ti $3d$ band occupation $n_{\mathrm{occ}}^{\mathrm{IF}}$ in the interface TiO_2 layer (within the muffin-tin sphere integrated between $\mathrm{E_F} - 0.5$eV to $\mathrm{E_F}$); total occupation of the Ti $3d$ band throughout STO $n_{\mathrm{occ}}^{\mathrm{tot}}$; work function Φ and p-type Schottky barrier of nM/2LAO/STO(001).

nM	$d_{M-\mathrm{O}}$	Δz Å	$n_{\mathrm{occ}}^{\mathrm{IF}}$ (e)	$n_{\mathrm{occ}}^{\mathrm{tot}}$ (e)	Φ (eV)	p-SBH
1Na	2.43	-0.12	0.05	0.22	3.39	2.3
1Al	1.97	-0.20	0.15	0.38	3.53	3.0
1Ti	2.00	-0.19	0.13	0.41	4.05	2.8
1Fe	2.02	-0.14	0.08	0.32	4.54	2.4
1Co	2.00	-0.11	0.07	0.30	4.74	2.3
1Pt	2.31	-0.08	0.04	0.16	5.59	2.2
1Cu	2.16	-0.07	0.03	0.18	5.36	2.2
1Ag	2.64	-0.04	0.02	0.12	5.02	1.8
1Au	3.05	0.00	0.00	0.01	5.94	0.8
0.5Ti	1.87	-0.14	0.11	0.38	2.96	2.5
1Ti	2.00	-0.19	0.13	0.41	4.05	2.8
2Ti	2.06	-0.18	0.12	0.16	4.05	2.8
3Ti	2.05	-0.17	0.13	0.47	4.37	2.8

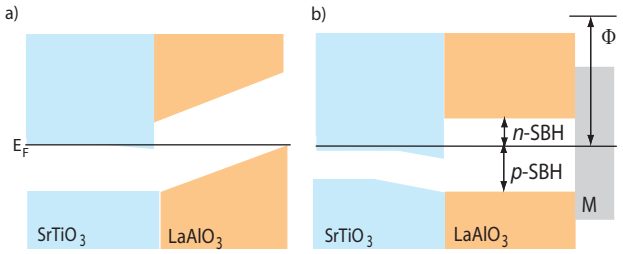

FIG. 8: Schematic band diagram of a) LAO/STO(001) at the verge of an electronic reconstruction at the critical LAO thickness; b) LAO/STO(001) covered by a metallic contact layer (M). Note, that the potential build up that leads to an electronic reconstruction in the uncovered LAO/STO(001) system at the critical thickness is strongly reduced/eliminated in M/LAO/STO(001) except for the case of noble metal electrodes.

also Table I) related to the size of the metal atom but also the bond strength.

Magnetism. In contrast to the noble metals, for Pt the $5d$ band is not completely occupied, and a spin-polarization of $0.49\mu_B$ results, as seen also in the case of Ti ($0.60\mu_{\mathrm{B}}$), another transition metal that is not magnetic in bulk. It is not uncommon for monolayers of even non-magnetic transition metals to show surface magnetism, since the reduced coordination narrows the bandwidth (see *e.g.* Ref.[50]). Analogously, the magnetic moments of the Fe ($2.94\mu_{\mathrm{B}}$) and Co ($2.01\mu_{\mathrm{B}}$) monolayers are enhanced w.r.t. the bulk values. However, even for these stronger magnets, when the STO substrate is thick no noticeable spin-polarization is induced in the 2DEG .

Structural relaxations. As already discussed for nTi/2LAO/STO(001) (see Section III), the presence of metallic contacts affects significantly the structural relaxations in LAO/STO(001). For the cases where the internal electric field within LAO is canceled (Al, Ti), the anion-cation buckling within LAO is small and of opposite sign to the uncovered film (see Fig. 7). For Fe, Co, Cu, Pt Δz switches sign and successively grows. Finally, Ag and Au show a lattice polarization within LAO of similar amount to the uncovered films. On the other hand, the occupation of the Ti $3d$ band at the LAO/STO interface is associated with a significant polarization in the STO substrate. The displacement between anions and cations is driven mainly by an outward oxygen shift and is largest in the interface TiO_2 layer (-0.20Å for an Al or Ti contact and vanishing for an Au contact) and decays in deeper layers away from the interface. This relaxation pattern resembles the one of n-type LAO/STO and LTO/STO superlattices[51,52].

A. Schottky barrier height and work function

The distinct mechanisms of formation of a 2DEG in LAO/STO(001) with and without a metallic contact are displayed in the schematic band diagram in Fig. 8. For LAO/STO(001) a thickness dependent MIT occurs as a result of the potential buildup, where the electronic reconstruction comprises both formation of holes at the surface and electrons at the interface[11,13]. In contrast, for M/LAO/STO(001) for $M =$ Na, Al, Ti, the potential in LAO is flat regardless of the LAO or STO thickness. Simultaneously, a 2DEG with higher carrier density is formed at the interface. For the late transition metals and especially for the noble metals, due to a weaker bonding and smaller/vanishing charge transfer to the oxide layer, a finite slope within LAO remains, consistent with the recently reported potential build up in Pt/LAO/STO(001)[32].

The Schottky barrier height (SBH) between the metal and the oxide film is an important quantity for electronics applications which depends critically on the type of metal, the chemical bonding characteristics and the work function (see *e.g.* Ref. [35]). The p-SBH determined from the LDOS varies from 3.0 eV (Al) to 0.8 eV (Au) (see Table I). The values for Al (3.0 eV) and Pt (2.2) eV are close to DFT-values obtained for Al and Pt on LAO(001)[37] (2.8 and 1.5 eV, respectively). We note that the absolute values of both the p- and especially the n-SBH are influenced by the band gap problem of GGA as well as the LAO thickness of only 2 MLs, however we concentrate here on the relative trends within the series of different metal contacts which are correctly reproduced. The conduction band offset between the contact and LAO (nSBH, which can be obtained as a difference between the experimental band gap of LAO (5.6 eV) and the p-type SBH) scales with the work function of the system that varies from 3.39 eV (Na) to 5.94 eV (Au). The conduction band alignment between LAO and STO whichis influenced by the formation of a Shottky barrier between M and LAO and shows also a strong variation.

V. EMERGENCE OF THE GLOBAL BAND LINEUP

This variation in the basic properties opens up the fundamental questions: what are the general principles and microscopic process that determine the band line-ups? A noteworthy observation is that Au has the largest work function of all the metals studied here (see Table I) and at the same time produces the only case where the Fermi level lies within the band gap of the STO. This suggests a picture how the overall electronic structure and band lineups emerge that is both consistent and predictive: due to the large work function of the Au contact, the Fermi level lies within the STO gap. As a consequence, no charge transfers from the metal contact layer to the interface and the potential buildup within LAO remains unchanged, even increases due to secondary effects.

For lower Φ, when the M layer is deposited, charge flows from the metal layer to the interface, thereby filling the Ti $3d$ conduction band until the M Fermi level coincides with that of the 2DEG at the IF. This rearrangement of charge can be quantified. If q amount of charge per IF cell is transferred from the M layer to the TiO_2 layer at the IF – a distance of around 2.5 LAO lattice parameters a – the change in potential is $\Delta V = q \times 2.5a/a^2 \approx 9.5\ q$ eV. For n_{occ} listed in Table I ΔV is of the order of 0-3 eV and corresponds remarkably well to the change in internal potential within LAO obtained self-consistently as well as the variation in work function within the class of M contacts that has been studied.

As the Fermi levels in the system align, the dipole at the IF is altered and band bending occurs within STO near the IF, as well as some feedback on the Schottky barrier and the work function. The lattice polarization within LAO that screens the internal field also reduces proportionally. While some secondary effects are difficult to quantify, the calculated results are consistent, quantitatively, with this process of stabilization of the overall band lineups and carrier densities. The basic design principle identified here is: use a low work function if a high carrier density 2DEG at the IF is desired. V.v., the carrier density can be reduced by increasing the work function of metal M on LAO to the limit of Au with its $\Phi \approx 6$ eV, where no carriers are transferred to the interface.

VI. SUMMARY

In summary, our DFT-results show that metallic contacts ultimately change the electrostatic boundary conditions by allowing transfer of charge to the interface. Despite analogies to the adsorption of hydrogen on LAO/STO(001)[23], there are notable differences (*e.g.* the strong dependence of the potential slope on coverage in the latter system). These differences emphasize not only the importance of the electrostatic boundary conditions[53] but also of a detailed knowledge of structural effects and chemical bonding to LAO/STO(001) in order to achieve better understanding and control device performance. The mechanisms identified here demonstrate that the choice of metal contact represents a further powerful means to tune the functionality at the LAO/STO(001) interface. Important outcomes of this study are in (i) predicting a broad variations in behavior at the M/LAO/STO(001) system for a representative series of simple, transition and noble metals used as electrodes, and (ii) identifying the the M/LAO work function as primary characteristic responsible for this variation.

Acknowledgments

We acknowledge discussions with J. Mannhart and financial support through the DFG SFB/TR80 (project C3) and grant *h0721* for computational time at the Leibniz Rechenzentrum. V. G. R. acknowledges financial support from CONACYT (Mexico) and DAAD (Germany). W. E. P. was supported by U.S. Department of Energy Grant No. DE-FG02-04ER46111.

* Electronic address: rossitzap@lmu.de

[1] A. Ohtomo and H. Y. Hwang, Nature **427**, 423 (2004).
[2] N. Reyren, S. Thiel, A. D. Caviglia, L. F. Kourkoutis, G. Hammer, C. Richter, C. W. Schneider, T. Kopp, A.-S. Retschi, D. Jaccard, et al., Science **317**, 1196 (2007).
[3] A. Brinkman, M. Huijben, M. van Zalk, J. Huijben, U. Zeitler, J. C. Maan, W. G. van der Wiel, G. Rijnders, D. H. A. Blank, and H. Hilgenkamp, Nature Mater. **6**, 493 (2007).
[4] D. A. Dikin, M. Mehta, C. W. Bark, C. M. Folkman, C. B. Eom, and V. Chandrasekhar, Phys. Rev. Lett. **107**, 056802 (2011).
[5] L. Li, C. Richter, J. Mannhart, and R. C. Ashoori, Nature Physics **7**, 762 (2011).
[6] J. A. Bert, B. Kalisky, C. Bell, M. Kim, Y. Hikita, H. Y. Hwang, and K. A. Moler, Nature Physics **7**, 767 (2011).
[7] S. Thiel, G. Hammerl, A. Schmehl, C. W. Schneider, and J. Mannhart, Science **313**, 1942 (2006).
[8] C. Cen, S. Thiel, G. Hammerl, C. W. Schneider, K. E. Andersen, C. S. Hellberg, J. Mannhart, and J. Levy, Nature Mater. **7**, 298 (2008).
[9] F. Bi, D. F. Bogorin, C. Cen, C. W. Bark, J.-W. Park, C.-B. Eom, and J. Levy, Appl. Phys. Lett. **97**, 173110 (2010).
[10] Y. Z. Chen, J. L. Zhao, J. R. Sun, N. Pryds, and B. G. Shen, Appl. Phys. Lett. **97**, 123102 (2010).
[11] R. Pentcheva, M. Huijben, K. Otte, W. E. Pickett, J. E. Kleibeuker, J. Huijben, H. Boschker, D. Kockmann, W. Siemons, G. Koster, et al., Phys. Rev. Lett. **104**, 166804 (2010).
[12] S. Ishibashi and K. Terakura, J. Phys. Soc. Jpn. **77**, 104706 (2008).
[13] R. Pentcheva and W. E. Pickett, Phys. Rev. Lett. **102**, 107602 (2009).
[14] R. Pentcheva and W. E. Pickett, J. Phys.: Condens. Matter **22**, 043001 (2010).
[15] W.-J. Son, E. Cho, B. Lee, J. Lee, and S. Han, Phys. Rev. B **79**, 245411 (2009).
[16] S. A. Pauli, S. J. Leake, B. Delley, M. Björck, C. W. Schneider, C. M. Schlepütz, D. Martoccia, S. Paetel, J. Mannhart, and P. R. Willmott, Phys. Rev. Lett. **106**, 036101 (2011).
[17] Y. Xie, C. Bell, T. Yajima, Y. Hikita, and H. Y. Hwang, Nano Lett. **10**, 2588 (2010).

[18] Y. Segal, J. H. Ngai, J. W. Reiner, F. J. Walker, and C. H. Ahn, Phys. Rev. B **80**, 241107(R) (2009).

[19] M. Sing, G. Berner, K. Go, A. Müller, A. Ruff, A. Wetscherek, S. Thiel, J. Mannhart, S. A. Pauli, C. W. Schneider, et al., Phys. Rev. Lett. **102**, 176805 (2009).

[20] S. A. Chambers, M. H. Engelhard, V. Shutthanandan, Z. Zhua, T. C. Droubaya, L. Qiao, P. V. Sushko, T. Feng, H. D. Lee, T. Gustafsson, et al., Surface Science Reports **65**, 317 (2010).

[21] Z. Zhong, P. X. Xu, and P. J. Kelly, Phys. Rev. B **82**, 165127 (2010).

[22] N. C. Bristowe, P. B. Littlewood, and E. Artacho, Phys. Rev. B **83**, 205405 (2011).

[23] W.-J. Son, E. Cho, J. Lee, and S. Han, J. Phys.: Condens. Matter **22**, 315501 (2010).

[24] P. R. Willmott, S. A. Pauli, R. Herger, C. M. Schlepütz, D. Martoccia, B. D. Patterson, B. Delley, R. Clarke, D. Kumah, C. Cionca, et al., Phys. Rev. Lett. **99**, 155502 (2007).

[25] L. Qiao, T. C. Droubay, V. Shutthanandan, Z. Zhu, P. V. Sushko, and S. A. Chambers, J. Phys.: Condens. Matter **22**, 312201 (2010).

[26] M. Huijben, A. Brinkman, G. Koster, G. Rijnders, H. Hilgenkamp, and D. H. A. Blank, Adv. Mater. **21**, 1665 (2009).

[27] H. Chen, A. M. Kolpak, and S. Ismail-Beigi, Adv. Mater. **22**, 2881 (2010).

[28] P. Zubko, S. Gariglio, M. Gabay, P. Ghosez, and J.-M. Triscone, Annu. Rev. Condens. Matter Phys. **2**, 141 (2011).

[29] J. Mannhart and D. G. Schlom, Science **327**, 1607 (2010).

[30] G. Cheng, P. F. Siles, F. Bi, C. Cen, D. F. Bogorin, C. W. Bark, C. M. Folkman, J.-W. Park, C.-B. Eom, G. Medeiros-Ribeiro, et al., Nature Nanotechnology **6**, 343 (2011).

[31] R. Jany, M. Breitschaft, G. Hammerl, A. Horsche, C. Richter, S. Paetel, J. Mannhart, N. Stucki, N. Reyren, S. Gariglio, et al., Appl. Phys. Lett. **96**, 183504 (2010).

[32] G. Singh-Bhalla, C. Bell, J. Ravichandran, W. Siemons, Y. Hikita, S. Salahuddin, A. F. Hebard, H. Y. Hwang, and R. Ramesh, Nature Physics **7**, 80 (2011).

[33] Z. Q. Liu, D. P. Leusink, W. M. Lü, X. Wang, X. P. Yang, K. Gopinadhan, A. Annadi, S. Dhar, Y. P. Feng, H. B. Su, et al., arXiv:1011.2629v1 (2010).

[34] A. Asthagiri and D. S. Sholl, J. Chem. Phys. **116**, 9914 (2002).

[35] M. Mrovec, J.-M. Albina, B. Meyer, and C. Elsässer, Phys. Rev. B **79**, 245121 (2009).

[36] A. Asthagiri and D. S. Sholl, Phys. Rev. B **73**, 125432 (2006).

[37] Y. F. Dong, Y. Y. Mi, Y. P. Feng, A. C. H. Huan, and S. J. Wang, Appl. Phys. Lett. **89**, 122115 (2006).

[38] N. Sai, A. M. Kolpak, and A. M. Rappe, Phys. Rev. B **72**, 020101(R) (2005).

[39] M. Stengel, D. Vanderbilt, and N. A. Spaldin, Phys. Rev. B **80**, 224110 (2009).

[40] C.-G. Duan, S. S. Jaswal, and E. Y. Tsymbal, Phys. Rev. Lett. **97**, 047201 (2006).

[41] M. Fechner, I. V. Maznichenko, S. Ostanin, A. Ernst, J. Henk, P. Bruno, and I. Mertig, Phys. Rev. B **78**, 212406 (2008).

[42] P. Blaha, K. Schwarz, G. Madsen, D. Kvasnicka, and J. Luitz, *Wien2k, an augmented plane wave plus local orbitals program for calculating crystal properties*, (Karlheinz Schwarz, Technische Universität Wien, Austria, 2001).

[43] J. P. Perdew, K. Burke, and M. Ernzerhof, Phys. Rev. Lett. **77**, 3865 (1996).

[44] V. I. Anisimov, I. V. Solovyev, M. A. Korotin, M. T. Czyżyk, and G. A. Sawatzky, Phys. Rev. B **48**, 16929 (1993).

[45] Z. S. Popović, S. Satpathy, and R. M. Martin, Phys. Rev. Lett. **101**, 256801 (2008).

[46] K. Janicka, J. P. Velev, and E. Y. Tsymbal, Phys. Rev. Lett. **102**, 106803 (2009).

[47] P. V. Ong, J. Lee, and W. E. Pickett, Phys. Rev. B **83**, 193106 (2011).

[48] A. F. Santander-Syro, O. Copie, T. Kondo, F. Fortuna, S. Pailhs, R. Weht, X. G. Qiu, F. Bertran, A. Nicolaou, A. Taleb-Ibrahimi, et al., Nature **469**, 189 (2011).

[49] W. Meevasana, P. D. C. King, R. H. He, S.-K. Mo, M. Hashimoto, A. Tamai, P. Songsiriritthigul, F. Baumberger, and Z.-X. Shen, Nature Mater. **10**, 114 (2011).

[50] R. Pentcheva and M. Scheffler, Phys. Rev. B **61**, 2211 (2000).

[51] R. Pentcheva and W. E. Pickett, Phys. Rev. B. **78**, 205106 (2008).

[52] S. Okamoto, A. J. Millis, and N. A. Spaldin, Phys. Rev. Lett. **97**, 056802 (2006).

[53] M. Stengel, Phys. Rev. Lett. **106**, 136803 (2011).